AIAA JOURNAL
Vol. 33, No. 10, October 1995

Sensitivity Study of Turbulent Reacting Flow Modeling in Gas Turbine Combustors

Xue-Song Bai* and Laszlo Fuchs†
Royal Institute of Technology, S-100 44 Stockholm, Sweden

The sensitivity of the flowfield to different models for the interaction between turbulence and combustion in a methane fired gas turbine combustion chamber has been studied numerically. The models studied here are the presumed probability density function method based on fast chemistry flame-sheet models, the eddy-dissipation concept model, and the presumed probability density function method with two versions of flamelet models. The mean velocity fields, the unburnt fuel, and the temperature distributions are relatively less sensitive to the different models and model parameters; however, the detailed distributions of species concentrations are fairly sensitive to different models and the model parameters. The sensitivity levels of the calculated quantities to model parameters are different for different levels of turbulence. In flows with highly intensive turbulence, the sensitivity level is relatively high for all of the models. This sensitivity is a limiting factor in applications where fine details are required. Comparisons between calculations and measurements are given.

I. Introduction

COMPUTATION of turbulent combustion in complex geometries, such as gas turbine combustion chambers, requires adequate treatment of the different processes: turbulence, chemical reactions, heat transfer, and the interaction among these processes. Turbulence has been studied extensively for nonreacting flows and has been found to be rather difficult to model. In principle, the turbulent flowfield can be computed by using direct numerical simulation of the Navier–Stokes equations and the other associated governing equations. It may be modeled in somewhat less detail by using large eddy simulations. Direct numerical simulations, however, are not yet applicable, due to limitations in computer capacity, for calculating turbulent combustion in complex geometries such as gas turbine combustors. Most of previous work has been based on the approach of further simplified turbulence models, such as the k–ϵ model.[1,2]

Chemical reactions involved in combustion consist of many elementary steps. A detailed study of all of the reaction steps involves a large number of species (and, consequently, also transport equations) and, hence, requires large computer memory and CPU times. As a result, reduced global reaction schemes are used.[3–5]

It is often accepted that most hydrocarbon oxidation processes are "fast" and that the combustion takes place in a thin layer (the so-called flamelet), whose thickness is in between the Kolmogorov microscale and the Taylor microscale. It is difficult to resolve such scales in practical numerical calculations, due to the limitation in computer capacity. Hence, there are several models proposed to simplify the mechanism of chemistry/turbulence interaction. One such model is based on the Burke–Schumann flame sheet approximation together with the probability density function (PDF) for describing the influence of turbulence. The model assumes that the reaction takes place in a zero thickness flame sheet. The model is believed to be appropriate for diffusion flames.[6] In turbulent flames, if the reaction time scale is shorter than that of turbulent mixing, the mixing would control the combustion process. The eddy dissipation concept[7] (EDC) and eddy breakup[8] models are based on this hypothesis. These models have widely been used and yield reasonable accuracy in a number of applications, including calculations of combustion in gas turbine combustors.[9] As shown in earlier applications,[10–12] however, the mentioned models have certain limitations; they are often either associated with nonuniversal, ad hoc, model constants or are limited to infinitely fast reaction chemistry (i.e., assuming mixed is burnt).

Increased interest in minor species such as NO_x requires models that can account for more detailed nonequilibrium chemistry. A model that can potentially account for more detailed chemistry without excessive increase in computational work and that also accounts for flame quenching due to large stretching is the flamelet model[13] (combined with a PDF accounting for effects of turbulence).

The aim of the present paper is to investigate the sensitivity of these different chemistry/turbulence interaction models in calculation of the combustion of methane in a gas turbine combustion chamber. We compare the results of different models with experimental data and study the dependence of the flame on the models and the associated model parameters. The turbulent flowfield is modeled using a two-equation k–ϵ model. The PDF is assumed to be a β function. Radiative heat transfer is taken into account via a discrete transfer method (DTM).[14] The calculations are based on a fully second-order finite difference scheme (second-order upwind for the convective terms and second-order central differences for the other terms). This is implemented in a defect-correction manner.[15]

II. Combustion Models

Combustion of hydrocarbons consists generally of hundreds of elementary reactions.[16] Numerical calculations using detailed chemistry for one-dimensional flames, such as the counterflow diffusion flame of methane combustion, have been reported.[17] As argued by Westbrook and Dryer,[3] however, for multidimensional and turbulent flows, a reduction of the large number of steps is needed. Such simplification will also suffice for many engineering applications. Several reduced global reaction mechanisms have been suggested.[3–5] In this paper we use a four-step mechanism of methane, which is obtained by the introduction of steady-state and partial equilibrium approximations to the elementary steps.[5] The mechanism consists of the following four reactions:

$$\begin{aligned} CH_4 + 2H + H_2O &\rightarrow CO + 4H_2 \\ CO + H_2O &\rightleftharpoons CO_2 + H_2 \\ 2H + M &\rightarrow H_2 + M \\ O_2 + 3H_2 &\rightleftharpoons 2H_2O + 2H \end{aligned} \tag{1}$$

Presented as Paper 94-0782 at the AIAA 32nd Aerospace Sciences Meeting, Reno, NV, Jan. 10–13, 1994; received Jan. 21, 1994; revision received March 8, 1995; accepted for publication March 9, 1995.

*Research Scientist, Department of Mechanics/Computational Fluid Dynamics; also Department of Heat and Power Engineering/Fluid Mechanics, Lund Institute of Technology, S-221 00 Lund, Sweden.

†Professor, Department of Mechanics/Computational Fluid Dynamics; also Department of Heat and Power Engineering/Fluid Mechanics, Lund Institute of Technology, S-221 00 Lund, Sweden. Member AIAA.

Different transport equations for the species mass fractions involved in the mechanism have to be solved. These equations have the following general form:

$$\frac{\partial \rho Y_i}{\partial t} + \frac{\partial \rho u_j Y_i}{\partial x_j} = \frac{\partial}{\partial x_j}\left(\rho D \frac{\partial Y_i}{\partial x_j}\right) + w_i \tag{2}$$

where ρ is density, t is time, and u_j are the velocity components in Cartesian coordinates x_j directions, respectively. Y_i is the mass fraction of species i, and w_i is the reaction rate of species i. D is the mass diffusivity. The Favre- (density weighted) averaged form of the equations is given by

$$\frac{\partial \bar{\rho}\tilde{Y}_i}{\partial t} + \frac{\partial \bar{\rho}\tilde{u}_j\tilde{Y}_i}{\partial x_j} = -\frac{\partial \bar{\rho}\widetilde{u_j''Y_i''}}{\partial x_j} + \frac{\partial}{\partial x_j}\left(\bar{\rho}D\frac{\partial \tilde{Y}_i}{\partial x_j}\right) + \bar{w}_i \tag{3}$$

where the overbar and the tilde denote the unweighted and the Favre averages, respectively. Two terms, i.e., the turbulent transport of species $-\bar{\rho}\widetilde{u_j''Y_i''}$ and the mean reaction rate $\bar{w}_i$, are unknown explicitly and have to be modeled. The turbulent transport fluxes may be modeled as in nonreacting flows.[18] Here, a gradient-diffusion model is used:

$$-\bar{\rho}\widetilde{u_j''Y_i''} = \frac{\mu_t}{Sc}\frac{\partial \tilde{Y}_i}{\partial x_j} \tag{4}$$

where μ_t is the eddy viscosity which is computed from the turbulent kinetic energy k and its dissipation rate ϵ,

$$\mu_t = C_\mu \bar{\rho} k^2/\epsilon \tag{5}$$

$C_\mu \sim 0.09$ is a model constant. The Schmidt number Sc is assumed to be 0.7.

The mean reaction rate is a result of turbulence/chemistry interactions; it is difficult to model due to its highly nonlinear dependence on the concentrations and the temperature. We shall apply the three types of models to account for the effects of turbulence in the following.

A. Model I: Probability Density Function Based on Unstretched Flame Sheets

The model assumes that the nonpremixed reaction takes place in a flame sheet with zero thickness, i.e., the chemical reactions are infinitely fast (mixed is burnt). The model neglects the effect of the flame environments, e.g., the effect of flame stretching. Thus, the model cannot account for local flame-quenching effects.

The mixture fraction Z is given by

$$Z = \frac{\phi - \phi_{,2}}{\phi_{,1} - \phi_{,2}}, \qquad \phi = Y_{\mathrm{fu}} - \frac{Y_{\mathrm{O}_2}}{r_{\mathrm{O}_2}} \tag{6}$$

Y_{fu} and Y_{O_2} are the fuel and oxygen concentrations, respectively, $r_{\mathrm{O}_2} = 4$ is the stoichiometric constant, and ϕ is an intermediate coupling function. Subscripts ,1 and ,2 denote the fuel and oxygen inlets conditions, respectively. By using the fact that the Lewis numbers for the major species are close to unity, the Favre-averaged mixture fraction equation can be written as

$$\frac{\partial \bar{\rho}\tilde{Z}}{\partial t} + \frac{\partial \bar{\rho}\tilde{u}_j\tilde{Z}}{\partial x_j} = \frac{\partial}{\partial x_j}\left(\frac{\mu_t + \mu_L}{Sc}\frac{\partial \tilde{Z}}{\partial x_j}\right) \tag{7}$$

where μ_L is the laminar viscosity. Z is a conserved scalar, and the direct calculation of the mean reaction rate is avoided. The species mass fractions are easily recovered from Z. Let $Z_{\mathrm{st}} = [-\phi_{,2}/(\phi_{,1} - \phi_{,2})]$, then the instantaneous quantities are related as follows:

$$Y_{\mathrm{fu}} = \begin{cases} (\phi_{,1} - \phi_{,2})Z + \phi_{,2}, & Z \geq Z_{st} \\ 0, & Z < Z_{st} \end{cases}$$

$$Y_{\mathrm{O}_2} = \begin{cases} -r_{\mathrm{O}_2}[(\phi_{,1} - \phi_{,2})Z + \phi_{,2}], & Z \leq Z_{st} \\ 0, & Z > Z_{st} \end{cases} \tag{8}$$

$$Y_{\mathrm{CO}_2} = r_{\mathrm{CO}_2}(ZY_{\mathrm{fu},1} - Y_{\mathrm{fu}})$$

$$Y_{\mathrm{H}_2\mathrm{O}} = r_{\mathrm{H}_2\mathrm{O}}(ZY_{\mathrm{fu},1} - Y_{\mathrm{fu}})$$

$$Y_{\mathrm{N}_2} = 1 - Y_{\mathrm{fu}} - Y_{\mathrm{O}_2} - Y_{\mathrm{CO}_2} - Y_{\mathrm{H}_2\mathrm{O}}$$

where $r_{\mathrm{CO}_2} = 2.75$ and $r_{\mathrm{H}_2\mathrm{O}} = 2.25$ are the stoichiometric constants. N_2 is a non-reacting dilution species. More detailed discussions can be found in Ref. 6.

A modification of this one-step reaction model is the use of equilibrium chemistry with more species. Here, to compare with other models, we use the equilibrium state derived from the four-reaction mechanism (1). In this model the species concentration is also a function of mixture fraction by assuming an adiabatic flame. We shall refer to the model using the one-step reaction as model Ia and to the one using equilibrium chemistry derived from Eq. (1) as model Ib.

The mean species concentrations can be computed through the PDF and the relations between species concentrations and the mixture fraction already described. This will be discussed further in Sec. II.D.

B. Model II: Eddy Dissipation Concept

Magnussen and Hjertager[7] have proposed the eddy dissipation concept to model the mean chemical reaction rate. When the chemical reaction takes place in a layer with thickness smaller than the finest scale (Kolmogorov scale), the mean chemical reaction depends on the mass transfer rate between the small eddies and their surrounding. In eddies of the order of the small-Kolmogorov scale, viscosity is important. The energy transferred from the large eddy into the small one may be modeled by the energy cascade theory.[19] Thus, the small-eddy scale may be estimated using the large-integral scale. As has been previously shown,[20] under the assumption that the various species are mixed homogeneously within the small eddies, the mean fuel consumption rate can be modeled by

$$\overline{w_{\mathrm{fu}}} = \bar{\rho}A \min\left(\tilde{Y}_{\mathrm{fu}}, \tilde{Y}_{\mathrm{O}_2}/r_{\mathrm{O}_2}\right)\epsilon/k \tag{9}$$

A is the model correction parameter, which depends on, among other factors, the fraction of the small eddies that are hot enough to take part in the reactions.[20] In their earlier paper, Magnussen and Hjertager[7] proposed $A = 4$ for the oxidation of C_2H_2 as global constants.

Applying the EDC model with mechanism (1) one has

$$\overline{w_{\mathrm{CH}_4}} = -R_1, \qquad \overline{w_{\mathrm{O}_2}} = -2R_1 - 16R_3$$

$$\overline{w_{\mathrm{CO}}} = (7/4)R_1 - R_2 \tag{10}$$

$$\overline{w_{\mathrm{H}_2}} = (1/8)R_1 + (1/14)R_2 - 2R_3$$

where

$$R_1 = A\bar{\rho}\min\left(\tilde{Y}_{\mathrm{CH}_4}, 0.5\tilde{Y}_{\mathrm{O}_2}\right)(\epsilon/k)$$

$$R_2 = A\bar{\rho}(\epsilon/k)\left[\min(\tilde{Y}_{\mathrm{CO}}, (14/9)\tilde{Y}_{\mathrm{H}_2\mathrm{O}}\right) - (7/11)(1/Kp_2)\min\left(\tilde{Y}_{\mathrm{CO}_2}, 22\tilde{Y}_{\mathrm{H}_2}\right)\Big]$$

$$Kp_2 = 0.035\exp(3652/\tilde{T})$$

$$R_3 = A\bar{\rho}(\epsilon/k)\min\left(\tilde{Y}_{\mathrm{H}_2}, (1/8)\tilde{Y}_{\mathrm{O}_2}\right)$$

Here, following Seshadri and Peters,[21] the H radical has been assumed to be in steady state. The numerical value of the model constant A will be discussed in Sec. IV.

C. Model III: Probability Density Function Based on Stretched Laminar Flamelets

When the reaction takes place in a thin layer, one can show that by introducing a Crocco type of coordinate transformation,[13] the leading term of the transport equation for species concentrations can be written as

$$\chi \frac{d^2 Y_i}{dZ^2} = -2w_i \tag{11}$$

in the vicinity of the flamelet region.

$$\chi = 2D \frac{\partial Z}{\partial x_j} \frac{\partial Z}{\partial x_j}$$

Based on model Ia as the outer structure and assuming a steady-state H-radical distribution, Seshadri and Peters[21] presented an asymptotical analysis for the diffusion flame of methane combustion. Three inner layers were suggested, i.e., a thin CH_4 consumption layer toward the fuel rich side in Z space, a thin CO, H_2 oxidation layer toward the lean side, and, in between, a thin nonequilibrium layer for the water gas shift reaction. In each layer, coordinate stretching based on the thickness of the layer was introduced. The dependent variables were expanded in terms of the thickness of the layer. For example, in a CH_4 consumption layer,

$$\eta = (Z - Z_0)/\delta_f, \qquad Y_i = y_i^0 + \delta_f y_i + \cdots \tag{12}$$

($i = CH_4, O_2, H_2, CO, H_2O, CO_2$) where η is the stretched coordinate, y_i is normalized dependent variable, and δ_f denotes the thickness of the CH_4 consumption layer. The superscript 0 denotes the condition $Z = Z_0$, where the CH_4 consumption layer is located.

Applying the asymptotical expansion to Eq. (11), the ordinary differential equation can be solved when χ^0 is given. The whole set of solution provides the flamelet library: $Y_i = Y_i^b(Z, \chi^0)$. The term χ^0 can influence the species concentration field (and, hence, the temperature) considerably. Since χ^0 represents the effect of stretching, the flamelet library takes into account the effect of flame quenching due to large stretching.[13] Namely, when χ^0 exceeds a critical value (the quenching limit, denoted by χ_q) no solution to Eq. (11) can be obtained. This corresponds to the state of inert mixing of fuel and oxidant. A relation between Y_i and Z [denoted by $Y_i^q(Z)$], when $\chi^0 > \chi_q$, is

$$\begin{aligned} Y_{CH_4} &= Z, & Y_{O_2} &= 0.233(1 - Z) \\ Y_i &= 0, & (i &= H_2O, CO_2, H_2, CO, H) \end{aligned} \tag{13}$$

It is interesting to note that, independent of how many steps and species are involved, only two independent variables (Z, χ^0) are needed. This is fairly advantageous when one introduces more detailed chemistry into the calculations.

Hereafter, we shall refer to the model using the Seshadri and Peters flamelet structure as model IIIa. By comparing computations with experimental data, a large difference between results computed using model IIIa and measurement is found, in particular in terms of CO and CO_2. We speculate that this deficit is due to the use of model Ia as the flamelet outer structure. Thus, a modified flamelet structure is suggested here, which will be referred to as model IIIb. The difference between models IIIb and IIIa is that the outer structure of model IIIb is model Ib, i.e., the equilibrium state as derived from the same reaction mechanism, Eq. (1). This is the consistent limit of the flamelet as the Damkolher number approaches infinity. In the inner flamelet structure, the H-radical consumption layer (on the oxygen-rich side) is solved whereas in the fuel consumption layer H is still assumed to be in steady state. Considerably different CO and CO_2 profiles are obtained using model IIIb as compared to those using model IIIa. As will be shown later, the modified model (IIIb) yields results that are closer to the measured data.

D. Modeling of the Probability Density Function

With the laminar flame structure $Y_i(Z, \chi^0)$ provided by the described methods, the mean thermochemical properties in turbulent reacting flows can be computed if the PDF is known, via

$$\tilde{Y}_i = \int_0^{\chi_q} \int_0^1 Y_i^b(Z, \chi^0) \wp(Z, \chi^0)\, dZ\, d\chi^0 + \int_{\chi_q}^{\infty} \int_0^1 Y_i^q(Z) \wp(Z, \chi^0)\, dZ\, d\chi^0 \tag{14}$$

Equation (14) can be interpreted as the ensemble average of the laminar flamelets in turbulent flows.[22] Peters[13] argued that often the flamelet is so thin that it can be treated as a laminar layer embedded inside the turbulent flowfield.

The equation for the joint PDF $\wp(Z, \chi^0)$ can be derived from the first principle.[23] Some terms, however, have to be modeled. Furthermore, solution of the $\wp(Z, \chi^0)$ equation will require large amount of CPU time and computer memory. A Monte-Carlo type method is usually used.[23] It is not uncommon to use the presumed PDF approach, which implies that the shape of the PDF is assumed. Here, the shape of the joint PDF $\wp(Z, \chi^0)$ is difficult to guess. The modeling problem may, however, be shifted via the identity

$$\wp(Z, \chi^0) = \wp_1(Z)\wp_2(\chi^0 \mid Z)$$

where $\wp_1(Z)$ is the PDF for Z; $\wp_2(\chi^0 \mid Z)$ is the conditioned PDF for a fixed value of Z. Thus, one can model $\wp_1(Z)$ and $\wp_2(\chi^0|Z)$ separately.

The most commonly used PDFs for the conserved scalar Z [$\wp_1(Z)$] are the β function and the clipped Gausian distribution. The β-function distribution is given by

$$\wp_1(Z) = \frac{Z^{a-1}(1 - Z)^{b-1}}{\int_0^1 Z^{a-1}(1 - Z)^{b-1}\, dZ} \tag{15}$$

The parameters a and b are determined from the mean value of Z (denoted by $\tilde{Z}$) and the second moment of the Favre-averaged fluctuation of Z, denoted by $\widetilde{Z''^2}$. The mean of Z can be calculated via Eq. (7).

The transport equation for $\widetilde{Z''^2}$ is as follows[18]:

$$\frac{\partial \bar{\rho} \widetilde{Z''^2}}{\partial t} + \frac{\partial \bar{\rho} \tilde{u}_j \widetilde{Z''^2}}{\partial x_j} = \frac{\partial}{\partial x_j}\left(\frac{\mu_t + \mu_L}{Sc} \frac{\partial \widetilde{Z''^2}}{\partial x_j}\right) + 2\frac{\mu_t}{Sc} \frac{\partial \tilde{Z}}{\partial x_j} \frac{\partial \tilde{Z}}{\partial x_j} - C_D \bar{\rho} \frac{\epsilon}{k} \widetilde{Z''^2} \tag{16}$$

where $C_D \sim 2$ is a model constant.

For isotropic turbulence, in analogy to Kolmogorov's third hypothesis,[24] the PDF of the viscous dissipation rate averaged over a volume of the characteristic dimension (between the Kolmogorov scale and the integral scale) is assumed to have a log-normal distribution. Hence, one may assume[13]

$$\wp_2(\chi^0 \mid Z) = \frac{1}{\chi^0 \sigma_\chi \sqrt{(2\pi)}} \exp\left\{-\frac{1}{2}\left[\frac{\ell n(\chi^0) - \mu}{\sigma_\chi}\right]^2\right\} \tag{17}$$

The mean and the standard deviation of the distribution can be determined in the following way[22]:

$$\sigma_\chi^2 \approx 0.5 \ell n\left(0.1 Re_t^{\frac{1}{2}}\right), \qquad Re_t = \rho k^2/\mu_L \epsilon$$
$$\mu = -\sigma_\chi^2/2 + \ell n(\tilde{\chi}^0) \tag{18}$$

The mass-averaged scalar dissipation rate is modeled by

$$\tilde{\chi}^0 = \begin{cases} C_\chi \dfrac{\epsilon}{k} \widetilde{Z''^2} & Z = Z_{st} \\ \tilde{\chi}_\perp^0, & Z \neq Z_{st} \end{cases} \tag{19}$$

where $\widetilde{\chi_\perp^0}$ denotes the value of $(C_\chi(\epsilon/k)\widetilde{Z''^2})$ frozen at $Z = Z_{st}$ on the same line normal to $Z = Z_{st}$ surface where the point of interest is located. This treatment is to account for the history influence of upstream flame quenching on the downstream flame. C_χ (~2) is a model constant.

III. Numerical Schemes

When the mean properties of the flowfield are of interest, as in many engineering applications, the Favre-averaged equations are used. For closing these equations one has to use a turbulence model (e.g., the k–ϵ equations). The governing equations can be written, in cylindrical coordinates, as follows:

$$\frac{\partial\bar{\rho}\psi}{\partial t}+\frac{1}{r}\frac{\partial\bar{\rho}\tilde{v}\psi}{\partial r}+\frac{1}{r}\frac{\partial\bar{\rho}\tilde{w}\psi}{\partial\theta}+\frac{\partial\bar{\rho}\tilde{u}\psi}{\partial x}=\frac{1}{r}\frac{\partial}{\partial r}\left(r\frac{\mu_L+\mu_t}{Pr}\frac{\partial\psi}{\partial r}\right)$$

$$+\frac{1}{r}\frac{\partial}{\partial\theta}\left(\frac{\mu_L+\mu_t}{rPr}\frac{\partial\psi}{\partial\theta}\right)+\frac{\partial}{\partial x}\left(\frac{\mu_L+\mu_t}{Pr}\frac{\partial\psi}{\partial x}\right)+S_\psi \qquad (20)$$

where x, r, and θ denote the axial, radial, and azimuthal directions, respectively. Also, $\tilde{u}$, $\tilde{v}$, and $\tilde{w}$ represent the Favre-averaged axial, radial, and azimuthal velocity components, respectively, and ψ represents any of the dependent variables ($\tilde{u}$, $\tilde{v}$, $\tilde{w}$, k, ϵ, $\tilde{Y}_i$, etc.). For the continuity equation $\psi = 1$. Pr is the Prandtl (Schmidt) number. For the momentum equations and the k transport equation, $Pr = 1$, whereas for the ϵ equation we take $Pr = 1.22$. For the energy equation and species mass-fraction equations $Pr = Sc = 0.7$.

Before solving the partial differential equations (20), we write Eq. (20) in strong conservative form. The discretization is done on a staggered grid. The components of the velocity vector are defined at the center of the corresponding cell side. Scalars are defined at the cell center. All terms with the exception of the convective terms are approximated by central differences. The convective terms in all of the equations are approximated by second-order upwind differences, implemented in a defect-correction manner. That is, the relaxation operator employs a hybrid approximation while the defect (i.e., that difference between the hybrid and the higher order operator) is computed at a previous iteration step and is applied as a given (source) term. Near solid (wall) boundaries central differences are used also for the convective fluxes.[15] To enhance stability of the iterative procedure a quasitime-marching technique[10,25] is employed. Details of the numerical method used here can be found in Refs. 10, 11, and 25.

The source term in the energy equation S_r is due to thermal radiation. S_r is calculated by assuming that the radiating medium is gray

$$S_r = \sigma_a\int_{4\pi} I_r\,\mathrm{d}\Omega - 4\sigma_a\sigma T^4 \qquad (21)$$

where σ_a is the absorption coefficients of the gas and σ is the Stefan–Boltzmann constant. I_r is the intensity of thermal radiation. The intensity I_r satisfies the following equation:

$$\frac{\mathrm{d}I_r}{\mathrm{d}s} = -\sigma_a I_r + \frac{\sigma_a\sigma T^4}{\pi} \qquad (22)$$

To calculate the radiative heat source term in the mean energy equation, the discrete transfer method[14] and a ray tracing technique for general curvilinear coordinates[26] are employed.

IV. Numerical Simulations

Two geometrical configurations have been studied. The first one is a cylindrical jet burner, which has been used in an experimental investigation of Owen et al.[27] Different models are then compared with the measured data. The second case is a gas turbine combustion chamber. Different levels of turbulence and their influence on the different models are examined. In both cases the fuel (methane) and air are supplied through different inlets.

A. Comparison of Different Models with Measurements

First, we consider the experimental rig of Owen et al.[27] The geometry can be seen from Fig. 1. The inlet fuel and air are supplied at a ratio of 0.05 (~1 m/s and 20 m/s, respectively). Inlet fuel/air equivalence ratio is 0.9, and inlet pressure is 3.9 atm. Air is supplied at 750 K. The inlet turbulence intensity is 15% and 20% for air and fuel inlets, respectively. These figures are obtained from comparing the calculations with the measured data at a near inlet location ($x/D = 0.052$, where D is the burner diameter). Further details of the setup may be found in Owen et al.[27] In the calculations, several different grids have been tested to minimize the uncertainties due to the numerical scheme. The final choice is a 102 × 62 × 3 grid in the axial, radial, and azimuthal directions, respectively. In the azimuthal direction, axisymmetry is assumed (as in the experimental device). In the computation, the model constants for models Ia, Ib, IIIa, and IIIb are those given in the Sec. II. The model constant A in model II is calibrated by comparison between computations and experiments. It is found that $A = 0.75$ gives close results to the experiments. The general validity of this value will be examined in Sec. IV.B.

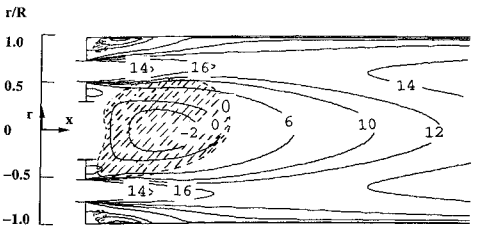

Fig. 1 Mean axial velocity contour in the experimental rig[27]: dashed line measured data, solid line model II (EDC, $A = 0.75$), shadow region recirculation region; locations of fuel and air inlets indicated in the left side of the figure; R (= $D/2$) radius of the burner.

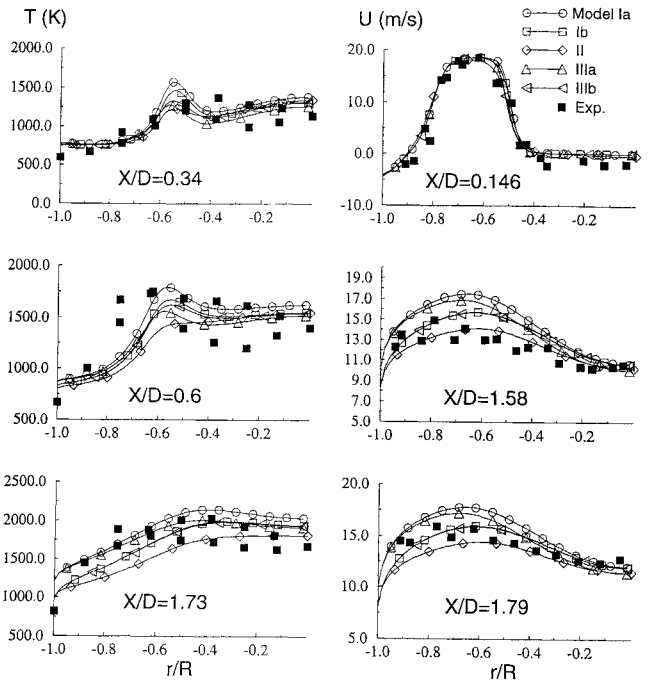

Fig. 2 Mean axial velocity component and temperature distributions along the radial direction at different axial stations.

The isocontours of the axial velocity component is also plotted in Fig. 1 (using model II). Certain differences between the computed results and measured data are observed. In particular, the size of the calculated recirculation zones differs from the measurements. This is partly due to the use of k–ϵ turbulence model. Higher order models could possibly improve the predictions, for the cost of longer computational time.

Figure 2 depicts the axial velocity profiles as computed using different models. It is shown, both in Figs. 1 and 2, that although there are differences between the calculated results and measurements, the differences are not too large; all models give results in the range of the measured data. The temperature profiles are also given in Fig. 2. As seen, the results as computed from different models are comparable to each other and in the range of experiment data.

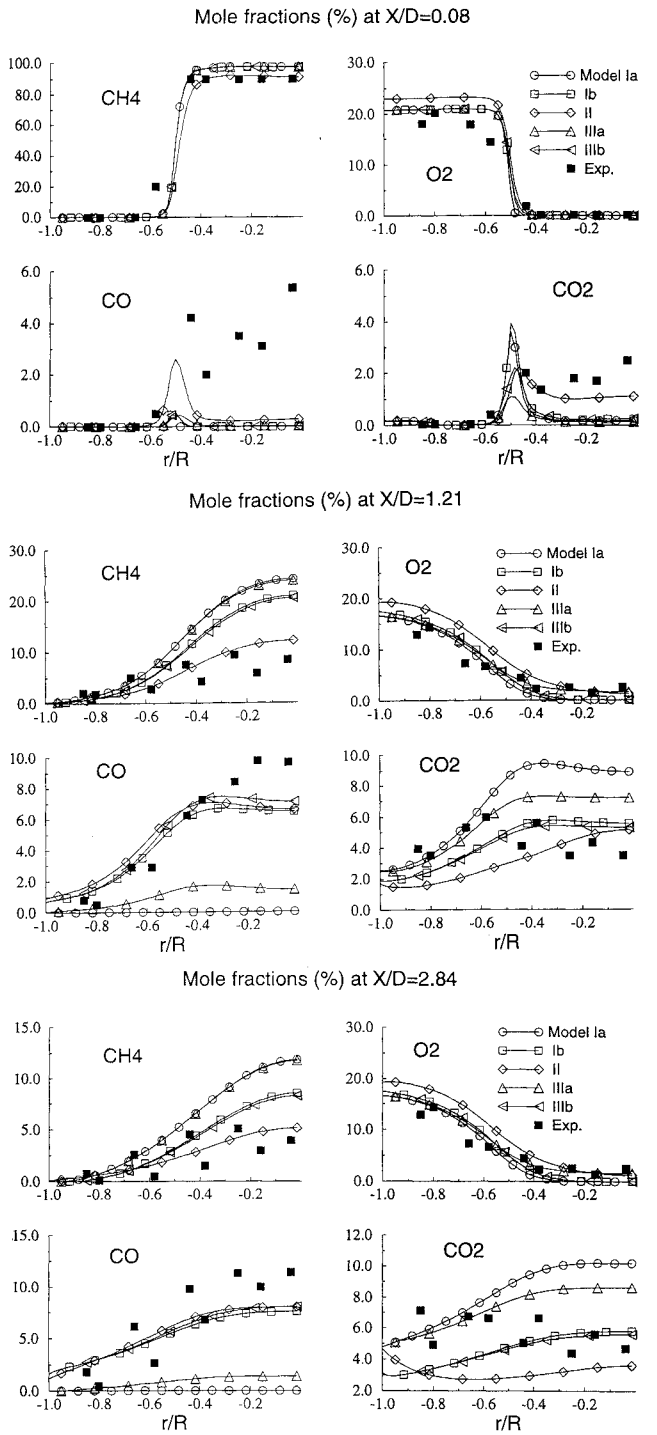

Fig. 3 Mean species mole fraction distributions along the radial direction at different axial stations.

When it comes to the prediction of the different species, there is a clear discrepancy between the predictions and the measured data. This discrepancy is larger for CO and CO_2 (Fig. 3). In the near inlet position ($x/D = 0.08$), both CO and CO_2 are underestimated by all of the models considered here. This difference could possibly be attributed to the sampling procedure in the measurements. The fuel and oxygen concentrations are well predicted by all of the models in this near inlet location. In downstream locations, e.g., $x/D = 1.21$ and $x/D = 2.84$, the differences in CO and CO_2 and fuel concentrations are large. It is shown that models Ib, II, and IIIb compare well with the experiments, whereas models Ia and IIIa agree less well. The results show that the influence of stretching on the flame is not large, so that the flamelet model is close to the large Damkolher number limit. Under such conditions models I and III should result in similar results. The difference in the results between models I and III can be attributed to the way chemistry and the flame-structure are

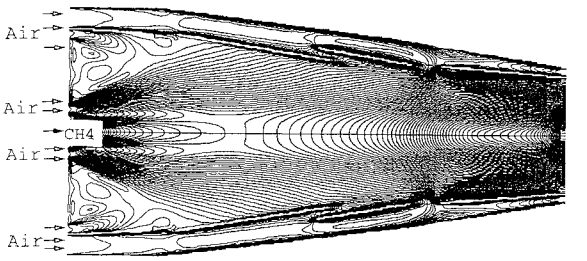

Fig. 4 Isocontours of the velocity field, computed using model II for the inlet turbulent intensity 20%.

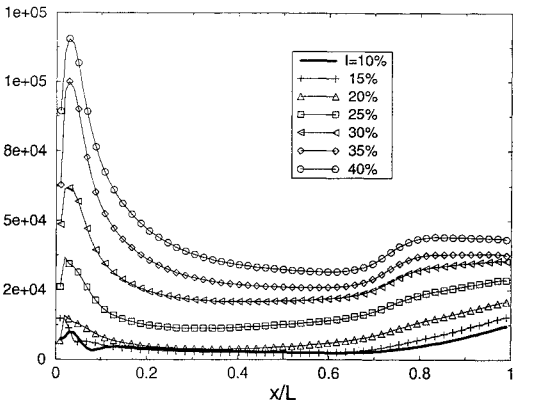

Fig. 5 Distribution of turbulent Reynolds number $\rho k^2/\mu_L \epsilon$ along the axis of the combustor for different levels of inlet turbulence; L is the length of the combustor.

treated. The results indicate that the flamelet structure of model IIIb is a genuine improvement and that the one-step, infinitely fast flame-sheet model yields a poor representation of the outer structure of the flamelet. The difference in oxygen concentrations, between calculations using different models are small; all models give acceptable results as compared with measured data.

To further examine the applicability of these different models we apply three of the models (models Ib, II, and IIIb) to the prediction of reacting flows in a gas turbine combustor.

B. Model Sensitivity in Different Levels of Turbulence

The following calculations have been carried out for a gas turbine combustion chamber geometry. The fuel (methane) is injected through the inlet near the central line with inlet velocity of 5.7 m/s. The primary air is injected with a velocity of 51 m/s. The equivalence ratio of the primary air and fuel is 0.968. The secondary air is supplied at a velocity of 15 m/s through near side-wall inlets and the liner holes. The overall equivalence ratio is 0.165. The inlet fuel and air are supplied at 300 K. The combustion chamber includes a liner containing a dilution air entrance and film-cooling arrangements. The geometry of the combustor is depicted in Fig. 4, where also the speed isocontours are plotted.

The number of grid points used in the calculations is determined by the required accuracy. This accuracy is estimated by solving the problem on several grids with different mesh size. To keep the grid number minimal without significant loss of accuracy, we use periodic boundary condition in the azimuthal direction based on the observation that the steady-state mean flowfield is axisymmetric. The mesh used has 3 grids in the azimuthal direction, 104 grids in the axial direction, and 92 grids in the radial direction. The iterations are stopped when the residuals of the discretized equations are reduced by five orders of magnitude.

To study the effects of turbulence on the combustion, different levels of inlet turbulence are investigated. The inlet turbulence intensity is varied from 10% to 40%; the mean velocity and other inlet parameters are kept unchanged. The inlet turbulence intensity is defined as $I = \sqrt{k}/\tilde{u}$; $\tilde{u}$ is the mean axial velocity at inlet. Figure 5 shows the distributions of turbulent Reynolds number Re_t [as defined in Eq. (18)], along the axis of the combustor for different levels of inlet turbulence.

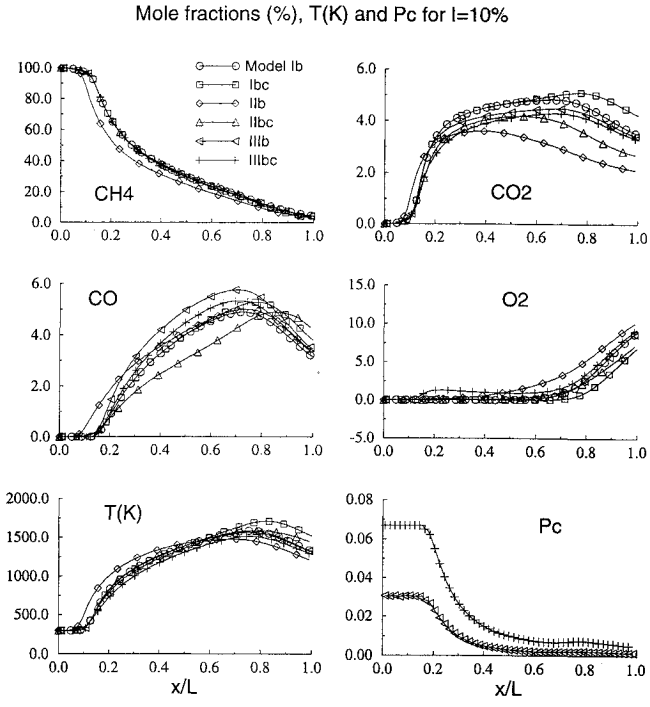

Fig. 6 Favre-averaged mean quantities as computed by different models, along the axis with inlet turbulence of I = 10%: Ib, model Ib with standard model constants; Ibc, model Ib with half the normal value of $\widetilde{Z''^2}$; IIb, EDC model with A = 0.75; IIbc, EDC model with A = 1.5; IIIb, model IIIb with standard model constants; and IIIbc, model IIIb with a lower quenching limit; Pc is the probability for flame quenching.

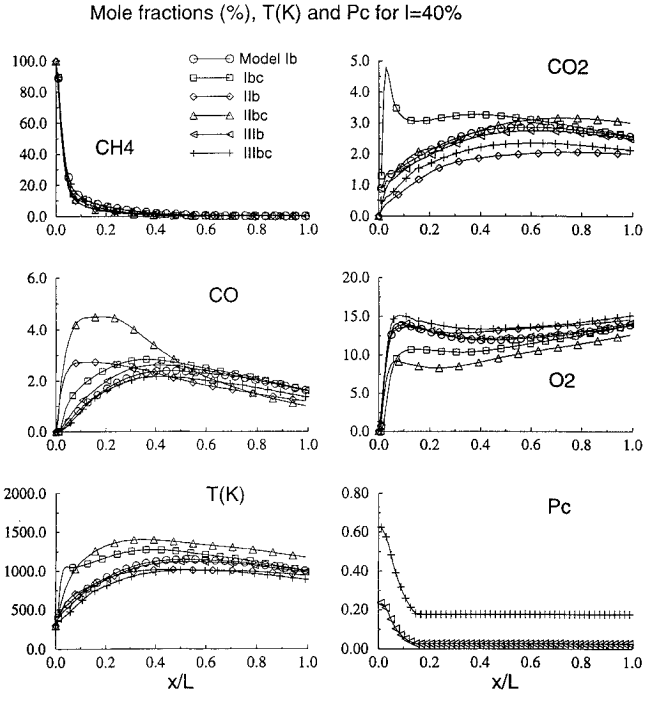

Fig. 7 Favre-averaged mean quantities as computed by different models, along the axis of the combustor, I = 40%; notation is the same as Fig. 6.

Higher levels of inlet turbulence intensity lead to higher levels of turbulence in the flowfield which implies higher level of mixing and larger eddy viscosity. Thus, the sensitivity of any model for accounting for turbulent/chemistry interaction will be inevitably dependent on the level of inlet turbulence.

Figures 6 and 7 show the distribution of different (Favre-averaged) quantities along the axis of the combustor as computed using different models for different levels of inlet turbulence. Figure 6 corresponds to results with a rather low level of inlet turbulence

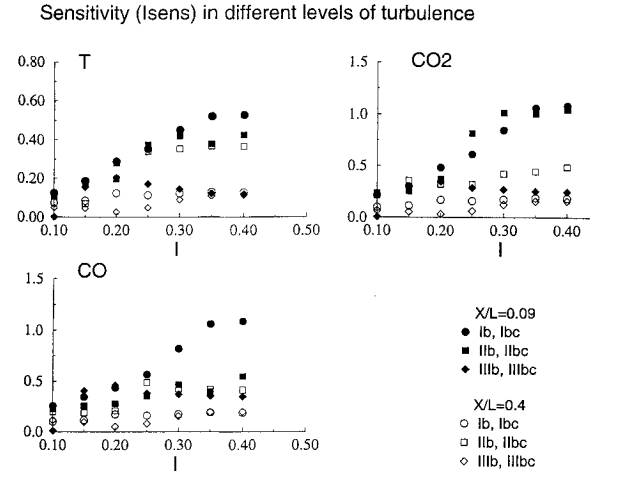

Fig. 8 Sensitivity of results to variations of parameters in different models at different levels of turbulence intensities; notation is the same as Fig. 6.

(I = 10%). The mixing of fuel and oxidant, with this level of turbulence, is insufficient. Hence, the fuel leakage at the combustor outlet is high (~10% in molar fraction at axis). To examine the sensitivity of results to the choice of model parameters, different model constants are used. In Fig. 6 (also in Figs. 7 and 8) Ib represents the flame sheet model Ib based on a β-function PDF and standard model constants. Ibc represents model Ib with its $\widetilde{Z''^2}$ only half of the value as computed from the standard version (model Ib). This difference is due to a bad calibration of the model constants in Eq. (16) or, equivalently, poor choice of the shape of the PDF. In particular, when $\widetilde{Z''^2} = 0$ the β function tends to a spike (δ function). IIb and IIbc represent the EDC model with A = 0.75 and with A = 1.5, respectively. IIIb represents the flamelet model based on the equilibrium state outer structure and β-function PDF. The quenching limit as computed by model IIIb is $\chi_q = 22.7\ s^{-1}$. For case IIIbc of Figs. 6–8, 10% of that χ_q value is used.

From Fig. 6, one can see that the fuel concentration is less sensitive to the choice of the particular model or the numerical values of the model constants. Other quantities exhibit considerably higher sensitivity. In particular, the results generated by using model II are more sensitive to the variations of model constants. The variation of model constants of model Ib yields moderate changes in the results; it is expected that the change in the shape of the PDF will lead to similar consequences. The results are fairly insensitive to the quenching limit of model IIIb. This is because the stretching rate in this low-level turbulence is rather low. The probability of local flame quenching Pc as defined by

$$Pc = \int_{\chi_q}^{\infty} \wp_2(\chi^0 \mid Z)\, d\chi^0$$

is less than 0.07 (Fig. 6). The Damkolher number is very large in this case; the chemistry is in near equilibrium and is far away from quenching conditions. Hence, as can be seen from Fig. 6, models IIIb and Ib give results close to each other. Since the flame is less stretched, we may expect that models Ib and IIIb will give reasonable results. Model IIb with A = 1.5 does give results close to those given by models Ib and IIIb, however, the model constant is changed from the one calibrated in Sec. IV.A where A = 0.75. This fact demonstrates a clear weakness of model II.

Figure 7 depicts the situation corresponding to the case in Fig. 6 but with a considerably higher level of inlet turbulence (I = 40%). With these inlet conditions the turbulence/chemistry interaction is stronger. The flame is thicker and is being stretched by the small eddies. When the flame near the inlet is locally quenched, the flame is lifted away from the inlet. This phenomena can not be modeled by models I and II. Model III has the possibility of accounting for local quenching. As seen from Figs. 6 and 7, in low level of turbulence, the quenching is less probable. The probability of local quenching increases with increasing level of turbulence.

Because of the intensive mixing of fuel and oxidant, the flame is shorter and the outlet fuel concentration is below 0.01% in mole fraction (Fig. 7). Because of strong mixing, the leakage of O_2 to the axis is large. Local quenching near the inlet also increases oxygen leakage to the fuel-rich zone near the axis. This can be observed in Fig. 7 as the rapid increase in O_2 concentration near the inlet.

We also note that model I (and, therefore, model III) is sensitive to the variations in $\widetilde{Z''^2}$ (thus, to the shape of the PDF). This sensitivity is stronger in terms of the CO and the CO_2 fields. The sensitivity level is higher as compared to low-level turbulence case (cf., Fig. 6).

The results also show that the flame is fairly sensitive to the variations of model constants in model II. CO concentrations differ by more than 40% when the model constant A is doubled.

The mean temperature field is less sensitive to the different models and model constants. However, the mean temperature also has an elevated level of sensitivity with increasing levels of turbulence. The mean density field and velocity field are less sensitive to the different models and model constants.

Figure 8 depicts the sensitivity of species concentrations (CO and CO_2) and temperature to variations of model parameters for different levels of turbulence at two axial positions ($x/L = 0.09$ and $x/L = 0.4$). The sensitivity measure is defined as follows:

$$I_{\text{sens}} = \int_s |f - fc|\,\mathrm{d}r \Big/ \int_s f\,\mathrm{d}r$$

where f and fc denote the quantities (mole fractions or temperature) in models Ib, IIb, IIIb and Ibc, IIbc, IIIbc, respectively. The integration is taken along the radial direction across the flame region.

As has already been discussed, when inlet turbulence intensity is large (>20%) the results are fairly sensitive to the variations of model parameters in different models. CO and CO_2 are more sensitive than temperature, CH_4, and O_2 fields are. The results are fairly sensitive to the variations of the parameters in the presumed PDF (e.g., the PDF shape) and also to the numerical value of the EDC-model parameter.

The sensitivity of results to the quenching limit increases as the level of turbulence increases; this effect is demonstrated in the figure for the $x/L = 0.4$ plane. At near inlet plane (i.e., $x/L = 0.09$), this sensitivity reaches its maxima for inlet turbulent intensity of 20%. When $I < 20\%$, the possibility of local quenching is small; whereas for $I > 20\%$, extensive mixing of the rich oxygen into this region reduces the effects of quenching (note that the overall fuel/air equivalence ratio is 0.165 in this case). It will be expected that when the global fuel/air ratio is closer to stoichiometric condition, the flame will be more sensitive to the quenching limit at high levels of turbulence intensity.

C. Discussion

The three models described have different features that should be taken into account when choosing one of them.

The influence of large stretching on flame quenching is not modeled by model I and model II. Model III accounts for the quenching effect through the scalar dissipations rate (χ^0) which determines the quenching extent. Therefore, χ^0 should include the history influence of the upstream flame quenching on the downstream flame. Two-point joint PDF may be used for the inclusion of this effect. Also, the influences of turbulence anisotropic and the chemical reactions on χ^0 could be modeled by a PDF. The PDF can be computed by using a transport equation (which contain certain terms that must also be modeled). Solving the PDF-transport equations implies longer computational times. In this respect, with few reactions taken into account, the computational time required by model III is longer than that required by model II; however, this situation may be reversed for a larger number of chemical reactions.

It may be also noted that model II implies less restrictions on the burner and flame configuration. In cases with multiple inlets and types of fuel, a single conserved scalar such as the mixture fraction, is not sufficient to describe the problem, therefore, models I and III require further modifications to the ones used in this paper.

The turbulent flowfield becomes more sensitive to the interaction between the fluid flow and the chemical reactions as the stretching rate close to the quenching limit. In such flow situations, the convergence of numerical calculations becomes slower for those approaches which model the mean reaction rates directly, such as model II. Also, as more species and reactions are incorporated, each with different time scale, the problem becomes stiff, which makes the numerical computations with model II more difficult. Models I and III avoid such difficulty by solving only the mixture fraction (a conserved scalar) and the dissipation rate of the mixture fraction, together with flame sheet or flamelet libraries.

Because of the increasing interest in reducing emissions and the increase in computational power, one may expect that more species and reactions will taken into consideration. In this respect, model I is not appropriate since the details of the nonequilibrium process have been neglected. Model II is associated with the difficulty of determining the model constants for each of the reactions. Model III could incorporate more species and reactions provided that the laminar flamelet library is known. Matched asymptotic analysis may be a feasible approach to obtain such a flamelet library.

V. Summary and Conclusions

Sensitivity study of the simulated mean quantities of different combustion/turbulence interaction models and different model parameters has been carried out. The calculations are performed in a methane-fired cylindrical burner and a gas turbine combustion chamber. The models used are the presumed PDF method with a one-step flame-sheet model (model Ia) or an equilibrium state chemistry derived from Peters' four-step global reaction mechanism (model Ib), the EDC model (model II), and the PDF method with a flamelet model with two variations: model IIIa, based on the one-step fast chemistry as the outer structure, and model IIIb, based on the equilibrium state chemistry as the outer structure. The presumed PDF is β function. Through study of the different models, we may conclude the following.

The sensitivity level of the results to different models and model parameters are fairly different. The mean unburnt fuel concentrations, the mean temperature, and the mean velocity fields are relatively less sensitive to the particular choice of models and model parameters. Detailed species concentrations, such as CO and CO_2 concentrations are, on the other hand, considerably more sensitive.

The sensitivity level of the results to model parameters is different for different levels of turbulence. In highly intensive turbulent flows, the results are more sensitive to model parameters for all three models. Model I, the flame sheet model based on the infinitely fast chemistry, will be adequate when the level of stretching and intensity of turbulence is low. In such a case, the flame sheet model based on one-step fast chemistry is not only unable to predict small species, such as CO, but also poor in calculation of major species, such as CO_2, compared to measurements. Model Ib, based on an equilibrium chemistry including more species, e.g., Peters' four-step chemistry, compares well with the measured data. Model I has no mechanism to account for the effect of stretching on local flame quenching. Therefore, its applicability to highly intensive turbulent flows is limited.

Model II may give results close the measurements. However, the sensitivity level of results to the numerical value of the model constant, is higher compared to other models. Since the model constants are not universal, the higher level of sensitivity to the numerical value of the model constant is a clear weakness. The model is also based on infinitely fast chemistry (assuming mixed is burnt); it will also be limited to flows with low level of turbulence, since it contains no mechanism to account for flame quenching.

Model III can qualitatively accommodate the effect of large stretching on flame quenching. With an equilibrium state as the outer limit of the flamelet structure, the model (IIIb) gives results comparable with measured data. The model is suitable for flows with both weak and moderate levels of turbulence. In flows with a high level of turbulence or when the flame is thick, the thin flamelet assumption is questionable and model IIIb may not be adequate.

Acknowledgment

This work is supported by NUTEK, the Swedish National Board for Industrial and Technical Development.

References

[1]Mellor, A. M., and Ferguson, C. R., "Practical Problems in Turbulent Reacting Flows," *Turbulent Reacting Flows*, edited by P. A. Libby and F. A. Williams, Vol. 44, Topics in Applied Physics, Springer–Verlag, New York, 1980, pp. 45–63.

[2]Lockwood, F. C., Papadopoulos, C., and Abbas, A. S., "Prediction of a Corner-Fired Power Station Combustor," *Combustion Science and Technology*, Vol. 58, Nos. 1–3, 1988, pp. 5–23.

[3]Westbrook, C. K., and Dryer, F. L., "Simplified Reaction Mechanisms for the Oxidation of Hydrocarbon Fuels in Flames," *Combustion Science and Technology*, Vol. 27, Nos. 1–2, 1981, pp. 31–43.

[4]Jones, W. P., and Lindstedt, R. P., "Global Reduced Scheme for Hydrocarbon Combustion," *Combustion and Flames*, Vol. 73, No. 3, 1988, pp. 233–249.

[5]Peters, N., "Numerical and Asymptotic Analysis of Systematically Reduced Reaction Schemes for Hydrocarbon Flames," *Lecture Notes in Physics*, Vol. 241, Springer–Verlag, New York, 1985, pp. 90–109.

[6]Bilger, R. W., "Turbulent Flows with Nonpremixed Reactants," *Turbulent Reacting Flows*, edited by P. A. Libby and F. A. Williams, Vol. 44, Topics in Applied Physics, Springer–Verlag, New York, 1980, pp. 66–114.

[7]Magnussen, B. F., and Hjertager, B. H., "On Mathematical Modeling of Turbulent Combustion with Special Emphasis on Soot Formation and Combustion," *16th Symposium (International) on Combustion*, Combustion Inst., Pittsburgh, PA, 1976, pp. 719–729.

[8]Spalding, D. B., "Concentration Fluctuations in a Round Turbulent Free Jet," *Chemical Engineering Science*, Vol. 26, No. 1, 1971, pp. 95–107.

[9]Nikjooy, M., So, R. M. C., and Peck, R. E., "Modeling of Jet- and Swirl Stabilized Reacting Flows in Axisymmetric Combustors," *Combustion Science and Technology*, Vol. 58, Nos. 1–3, 1988, pp. 135–153.

[10]Bai, X. S., and Fuchs, L., "Calculation of Turbulent Combustion of Propane in Furnaces," *International Journal of Numerical Methods in Fluids*, Vol. 17, No. 3, 1993, pp. 221–239.

[11]Bai, X. S., and Fuchs, L., "Modeling of Turbulent Reacting Flows Past Bluff Bodies: Assessment of Accuracy and Efficiency," *Computers and Fluids*, Vol. 23, No. 3, 1994, pp. 507–521.

[12]Lin, C. S., "Numerical Calculations of Turbulent Reacting Flow in a Gas Turbine Combustor," NASA TM 89842, April 1987.

[13]Peters, N., "Laminar Diffusion Flamelet Models in Nonpremixed Turbulent Combustion," *Progress in Energy and Combustion Science*, Vol. 10, No. 3, 1984, pp. 319–339.

[14]Shah, N. G., "New Method of Computation of Radiation Heat Transfer in Combustion Chamber," Ph.D. Thesis, Dept. of Mechanical Engineering, Imperial College, London, 1979.

[15]Thakur, S., and Shyy, W., "Some Implementational Issues of Convection Schemes for Finite Volume Formulation," *Numerical Heat Transfer*, Pt. B, Vol. 24, No. 1, 1993, pp. 31–55.

[16]Warnatz, J., "Rate Coefficients in the C/H/O System," *Combustion Chemistry*, edited by W. C. Cardiner Jr., Springer–Verlag, New York, 1984, pp. 197–360.

[17]Dixon-Lewis, G., David, T., Gaskell, P. H., Fukutani, S., Jinno, H., Miller, J. A., Kee, R. T., Smooke, M. D., Peters, N., Effelsberg, E., Wannatz, J., and Behrendt, F., "Calculation of the Structure and Extinction Limit of a Methane-Air Counter Flow Diffusion Flame in the Forward Stagnation Region of a Porous Cylinder," *20th Symposium (International) on Combustion*, Combustion Inst., Pittsburgh, PA, 1984, pp. 1893–1904.

[18]Jones, W. P., and Whitelaw, J. H., "Calculation Methods for Reacting Turbulent Flows: a Review," *Combustion and Flame*, Vol. 48, No. 1, 1982, pp. 1–26.

[19]Tennekes, H., and Lumley, J. L., *A First Course in Turbulence*, 13th printing, MIT Press, Cambridge, MA, 1990, Chap. 8.

[20]Brostrom, M. F., "Time Dependent Numerical Calculation of Pool Fire Development in Enclosed Space," Ph.D. Thesis, Div. of Thermodynamics, Norwegian Inst. of Technology, Trondheim, Norway, Aug. 1987.

[21]Seshadri, K., and Peters, N., "Asymptotic Structure and Extinction of Methane-Air Diffusion Flames," *Combustion and Flame*, Vol. 73, No. 1, 1988, pp. 23–44.

[22]Liew, S. K., Bray, K. N. C., and Moss, J. B., "A Stretched Laminar Flamelet Model of Turbulent Nonpremixed Combustion," *Combustion and Flame*, Vol. 56, No. 2, 1984, pp. 199–213.

[23]Pope, S. B., "Computations of Turbulent Combustion: Progress and Challenges," *23rd Symposium (International) on Combustion*, Combustion Inst., Pittsburgh, PA, 1990, pp. 591–612.

[24]Kolmogorov, A. N., "A Refinement of Previous Hypothesis Concerning the Local Structure of Turbulence in a Viscous Incompressible Fluid at High Reynolds Number," *Journal of Fluid Mechanics*, Vol. 13, May 1962, pp. 82–85.

[25]Bai, X. S., and Fuchs, L., "A Multigrid Method for Calculation of Turbulence and Combustion," *Multigrid IV*, edited by P. W. Hemker and P. Wesseling, International Series of Numerical Mathematics, Vol. 116, 1994, pp. 131–142.

[26]Bai, X. S., and Fuchs, L., "Numerical Computation of Turbulent Combustion and Thermal Radiation in Gas Turbine Combustion Chambers," International Council of the Aeronautical Sciences, ICAS Paper 94-6.6.1, Sept. 1994.

[27]Owen, F. K., Spadaccini, L. J., and Bowman, C. T., "Pollutant Formation and Energy Release in Confined Turbulent Diffusion Flames," *16th Symposium (International) on Combustion*, Combustion Inst., Pittsburgh, PA, 1976, pp. 105–117.